A MODEL OF THE DRIFT OF NORTHERN ANCHOVY, *ENGRAULIS MORDAX*, LARVAE IN THE CALIFORNIA CURRENT

JAMES H. POWER[1]

ABSTRACT

The drift of northern anchovy, *Engraulis mordax*, larvae in the California Current to unfavorable offshore areas may be an important factor contributing to larval mortality, and hence it may affect recruitment and subsequent adult population size. A simulation model based on a finite-difference approximation to the advection-diffusion equation was developed to aid in the study of larval anchovy drift. Model components included the long-term mean geostrophic and wind-driven current velocities to 50 m depth, and turbulent diffusion. The model predicted larval distributions in the Southern California Bight and offshore regions after 30 days of drift, and these distributions were used to assess the extent of cross-shore and alongshore larval transport that occurs when spawning takes place at different locations, seasons, and during times of increased offshore-directed Ekman transport.

Offshore transport was minimal in most simulations. Simulations of drift starting from the location of peak spawning showed strongest seasonal effects, with currents during the season of peak northern anchovy spawning (March) resulting in reduced offshore dispersal when compared with currents at other times of the year. March currents also produced the greatest downshore (southeasterly) transport of larvae, and strong seasonal currents, such as the nearshore, northwesterly flowing California Countercurrent, can greatly affect the alongshore 30-day larval distributions. Offshore directed Ekman transport, associated with upwelling, does not strongly affect the drift of larvae in the nearshore region, but large increases in overall Ekman transport, or extension of spawning into offshore regions, can result in significant seaward transport of larvae out of the Southern California Bight.

The total population of northern anchovy, *Engraulis mordax*, a common pelagic fish off the west coast of North America, is comprised of three subpopulations (Vrooman et al. 1981): northern (found north of lat. 36°30'N); central (between lat. 29° and 38°N); and southern (south of lat. 29°N). The central subpopulation inhabits the Southern California Bight region, and in recent times has exhibited substantial changes in population biomass (e.g., Smith 1972). Analysis of northern anchovy scales deposited in sediments indicates that large northern anchovy population fluctuations have also occurred in the past few centuries (Soutar and Isaacs 1974). Historically the central subpopulation of northern anchovy has supported a significant fishery (Messersmith and Associates 1969; Sunada 1975; Stauffer and Charter 1982), and although the U.S. fishery has recently declined, there is still a significant Mexican fishery. The northern anchovy fishery, the recent and historical changes in anchovy population size, and the fish's important role in the marine ecosystem all provide the motivation for studying the mechanisms that may cause interannual variations in northern anchovy stock size.

Such changes in stock size may be a consequence of variations in the previous spawning stock size, or they can also arise as a result of interannual differences in mortality during prerecruit life history stages (Rothschild et al. 1982). Because the egg and larval stages have the highest mortalities, it seems possible that processes affecting the relative mortality during these stages can have a significant effect on subsequent recruitment. Two major causes of larval mortality are starvation and predation (Smith and Lasker 1978; Hunter 1981). A factor that may contribute to these is larval drift. The northern anchovy eggs and larvae, lacking adequate motility, can be involuntarily transported away from nearshore spawning areas. It is the nearshore regions in the Southern California Bight that most frequently contain adequate food concentrations for growth and survival of first feeding northern anchovy larvae (Lasker 1978, 1981).

Although eddies and other short-term mesoscale features are important in the Southern California Bight (Mooers and Robinson 1984; Simpson et al. 1984), the broad and relatively slow equatorward flow termed the California Current is the dominant feature in the region that persists on evolutionary

[1]Southwest Fisheries Center La Jolla Laboratory, National Marine Fisheries Service, NOAA, P.O. Box 271, La Jolla, CA 92038; present address: Coastal Fisheries Institute, Center for Wetland Resources, Louisiana State University, Baton Rouge, LA 70803-7503.

Manuscript accepted September 1985.
FISHERY BULLETIN: VOL. 84, NO. 3, 1986.

time scales. Hence, it seems plausible that northern anchovy spawning strategies have developed in response to the relatively predictable seasonal and spatial trends in the California Current. Possible relationships between time and location of fish spawning and the currents off the west coast of North America have been discussed by Parrish et al. (1981). They noted that in the Southern California Bight the Ekman (wind-driven) currents are generally diminished relative to other areas along the coast. This reduced offshore transport is favorable for the retention of fish eggs and larvae. However, some weak offshore directed Ekman transport is consistently present in the Southern California Bight year round (Nelson 1977; Parrish et al. 1981; Bakun and Parrish 1982).

Smith (1972) analyzed historical records of northern anchovy larval distribution in the Southern California Bight and found that samples taken farther offshore had a higher proportion of older larvae than that of samples taken nearshore. Assuming a uniform spatial and temporal distribution of spawning, this result implied that a significant fraction of northern anchovy eggs and larvae were transported offshore after nearshore spawning. Bailey (1981) found that the average distance offshore of Pacific hake, *Merluccius productus*, larvae north of Point Conception was positively correlated with offshore Ekman transport and that the magnitude of subsequent Pacific hake recruitment was negatively correlated with offshore transport. Hewitt and Methot (1982) compared the distributions of northern anchovy larvae sampled in 1978 and 1979 and found that the bulk of the larvae in 1979 were farther offshore than those in 1978 and that mortality of 0-group northern anchovy was greater in 1979 when compared with those spawned in 1978. The year 1979 was one of enhanced upwelling and colder temperatures (both concomitants of offshore Ekman transport) relative to 1978.

The studies cited above suggest drift may play an important role in larval ecology, but the conclusions drawn from plankton sampling must be viewed with caution. Inferences drawn from field collections about the drift of larvae usually carry the assumption that both northern anchovy spawning and larval mortality were uniform in space and time, because the time and distance scales involved largely preclude synoptic sampling of eggs and larvae throughout the region. Hence, only correlative explanations for the observed distribution can be made, and other causal factors affecting the larval distribution may be hidden. For example, an observation of greater proportions of older larvae in offshore waters could also result from earlier spawning or greater early mortality (possibly coupled with increased spawning activity) in those waters, and not drift. Additionally, the mesoscale variability present in the Southern California Bight and the considerable patchiness of early and late larvae (due to northern anchovy schooling behavior; Hewitt 1980, 1981a) further confound the conclusions drawn from plankton samples and diminish the value of interannual comparisons. Therefore, as an alternative to field studies, a simulation model of northern anchovy drift in the California Current was developed to help evaluate the role of drift in larval ecology. The objective was to use the model to determine the effect of differences in northern anchovy spawning location and time on the subsequent larval distribution and to evaluate the effects on larval distribution when offshore Ekman transport is increased above its normal mean value.

METHODS

The drift simulation was based on the two-dimensional (x,y) form of the advection-diffusion equation:

$$\frac{\partial F}{\partial t} + \frac{\partial}{\partial x}\left(uF - K_x\frac{\partial F}{\partial x}\right) + \frac{\partial}{\partial y}\left(vF - K_y\frac{\partial F}{\partial y}\right) = 0$$

where F = the concentration of eggs and larvae;
u and v = current velocities in the respective x and y directions; and
K_x and K_y = eddy diffusivity coefficients for the x and y directions.

An analytical solution to this equation cannot be evaluated relative to northern anchovy larval drift in the California Current, although a numerical approximation that specifies larval concentration as a function of location and time can be determined. This was accomplished by approximating each of the derivatives in the equation by weighted finite-differences, so that the model was algebraically formulated as the current and diffusivity-mediated fluxes of larvae among geographic points in the Southern California Bight. Apart from the assumption that larvae continually maintained themselves in surface waters, the northern anchovy were assumed to be conservative and completely passive drifters, i.e., no mortality or movement due to larval swimming was incorporated into the model. Details of the numerical methods used are presented in Power (1984).

The geographic grid for the model was defined

using the California Cooperative Oceanic Fisheries Investigation (CalCOFI) coordinate system. The CalCOFI grid is a regular coordinate system of cross-shore "lines" and alongshore "stations". The model and CalCOFI grids are oriented with respect to the coast so that increasing station number corresponds to increasing offshore distance and increasing line number implies the downshore (southeasterly) direction. Each line unit increment is spaced 12 nm apart, and each station unit represents 4 nm. The grid for the model was defined to form cells that were 37 km (20 nm) on a side, and the fluxes of larvae were among grid cell centers. Model coverage was from CalCOFI lines 70 to 120, and extended offshore to CalCOFI station 120 (Fig. 1).

Unless northern anchovy utilize a strategy whereby spawning is initiated in response to the presence of an eddy or other short-term mesoscale features, it can reasonably be expected that spawning time and location have evolved partially in response to predictable current features. For this reason, seasonal currents based on interannual means were used in the model. Northern anchovy spawning behavior relative to eddies, etc., is presently unknown, and there are persistent seasonal trends in spawning, e.g., northern anchovy spawn throughout the year, but March is typically the peak time of spawning (Smith 1972; Methot 1981).

Geostrophic currents for the model were calculated using the geopotential anomalies computed by Lynn et al. (1982). Lynn et al. used CalCOFI data collected between 1950 and 1978 to compute the average geopotential anomaly relative to 500 m for four seasonal periods (nominally January, April, July, and October) at 175 locations in the California Current. Average geopotential anomalies were computed for an additional 23 locations for this study to augment the Lynn et al. (1982) coverage

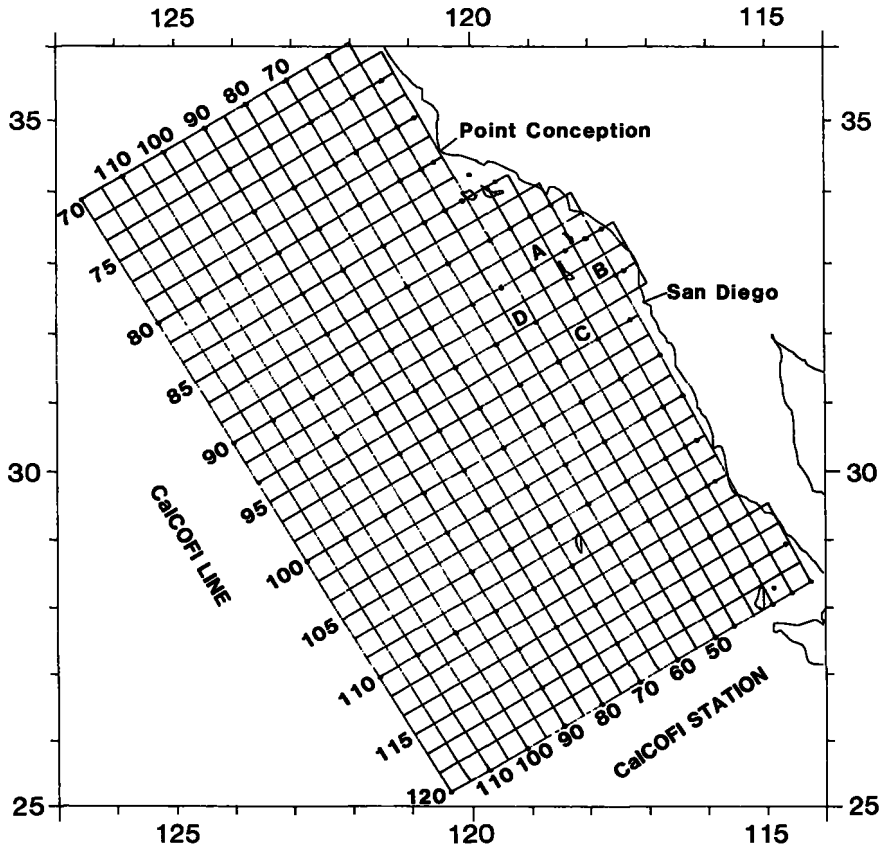

FIGURE 1.—Geographic grid used in the northern anchovy drift simulations, and the corresponding CalCOFI line and station coordinate system. Lettered locations are starting points for simulation presented in this paper. Mean geopotential anomolies (used for computing geostrophic currents) were calculated for the locations indicated by dots (Lynn et al. 1982; this study).

(Fig. 1). The top 50 m of the water column is the predominant depth range of anchovy larvae (Ahlstrom 1959), therefore mean anomaly values for the surface and for 10, 20, 30, and 50 m of depth were used in this study. The anomalies at each standard depth were interpolated to model grid nodes using the bivariate interpolation algorithm of Akima (1978). Geostrophic current velocities normal to each grid cell interface were computed for each of the standard depths, and average geostrophic current velocities were then calculated for a layer extending from the surface to 50 m.

Wind speed and direction data used in this study were from the data base summarized and discussed by Nelson (1977). The raw wind observations were converted to surface wind stress (τ) values using the relation

$$\tau = \rho C_d W^2$$

where ρ = air density (1.22 kg m^{-3});
C_d = drag coefficient; and
W = wind speed.

The drag coefficient was computed as a function of wind speed using the empirical relation of Amorocho and DeVries (1980, 1981). The computed wind stress vectors were partitioned by month of observation and resolved into alongshore and cross-shore components. A monthly mean wind stress component for each model grid cell interface was then computed by averaging the appropriate component of the stress vectors in the 37 km by 37 km area bisected by the grid cell interface. Total Ekman or wind-driven transport in the direction 90° to the right of the wind can be approximated by dividing the wind stress by the Coriolis parameter (Neumann and Pierson 1965), and this calculation was performed for the mean wind stress components. The mixed layer depth in the California Current is seldom >50 m, and is often <20 m in the Southern California Bight during the summer (Husby and Nelson 1982). It was assumed that Ekman transport occurring deeper than 50 m was negligible, and the Ekman transport values were converted to a mean wind-driven velocity for the surface to 50 m layer by dividing the transport by the 50 m layer thickness.

The final current velocities were calculated as the vector sum of the seasonal geostrophic and appropriate monthly Ekman components. Vector addition of the two components appears to be a reasonable assumption (Parrish et al. 1981), and no compensation for redistribution of mass owing to sustained winds was performed. The final seasonal current fields for the simulations were January, March (April geostrophic velocities plus March Ekman velocities), July, and October currents.

Figure 2 illustrates the general trends in the California Current for the January and March seasons. This figure should be interpreted with caution. Apart from the large potential differences between actual synoptic conditions and the average pattern used in the simulations, the resultant vector for a cell was necessarily computed for Figure 2 by averaging the current components of opposing cell faces and then calculating the resultant. A distortion is introduced wherever components on opposite faces of a cell differ in magnitude or sign, so that Figure 2 best represents features of the California Current that are consistent over several model grid cells. The California Current is evident as two regions of intensified southeasterly flow at the left margins and midlines of the plots. During all parts of the year except spring, the current turns toward shore at the southern end of the Southern California Bight. A northwesterly flow near the coast subsequently forms the inshore portion of a large cyclonic eddy (the Southern California Eddy; Owen 1980) that occupies most of the Southern California Bight. During most of the year part of this eddy's northeasterly flow continues past Point Conception, to form the California Countercurrent (Hickey 1979; Fig. 2, January plot). In the spring the southeasterly flow of the California Current moves closer to shore to obliterate the surface portion of the Countercurrent (Fig. 2, March). Tsuchiya (1980, fig. 2) gives a clear picture of the seasonal inshore-offshore movements of the California Current at CalCOFI lines 90 and 93. Close to shore in the southern half of the modeled region there is another region of intensified southeasterly flow, most evident in the March current plot. Lynn et al. (1981) provided detailed illustrations of the geostrophic flow regimes used in the simulations, and Nelson (1977) presented graphical representations of the wind stress fields along the west coast of North America. Hickey (1979) presented a comprehensive review of seasonal and spatial variations of the California Current and the possible driving mechanisms involved, and Owen (1980) reviewed the incidence and ecological consequences of eddies in the California Current system.

Two additional current fields were calculated in order to assess the effects of increased offshore directed Ekman transport on larval northern anchovy distribution. As mentioned earlier, the mean wind stress is consistently directed downshore during March in the modeled region, a condition

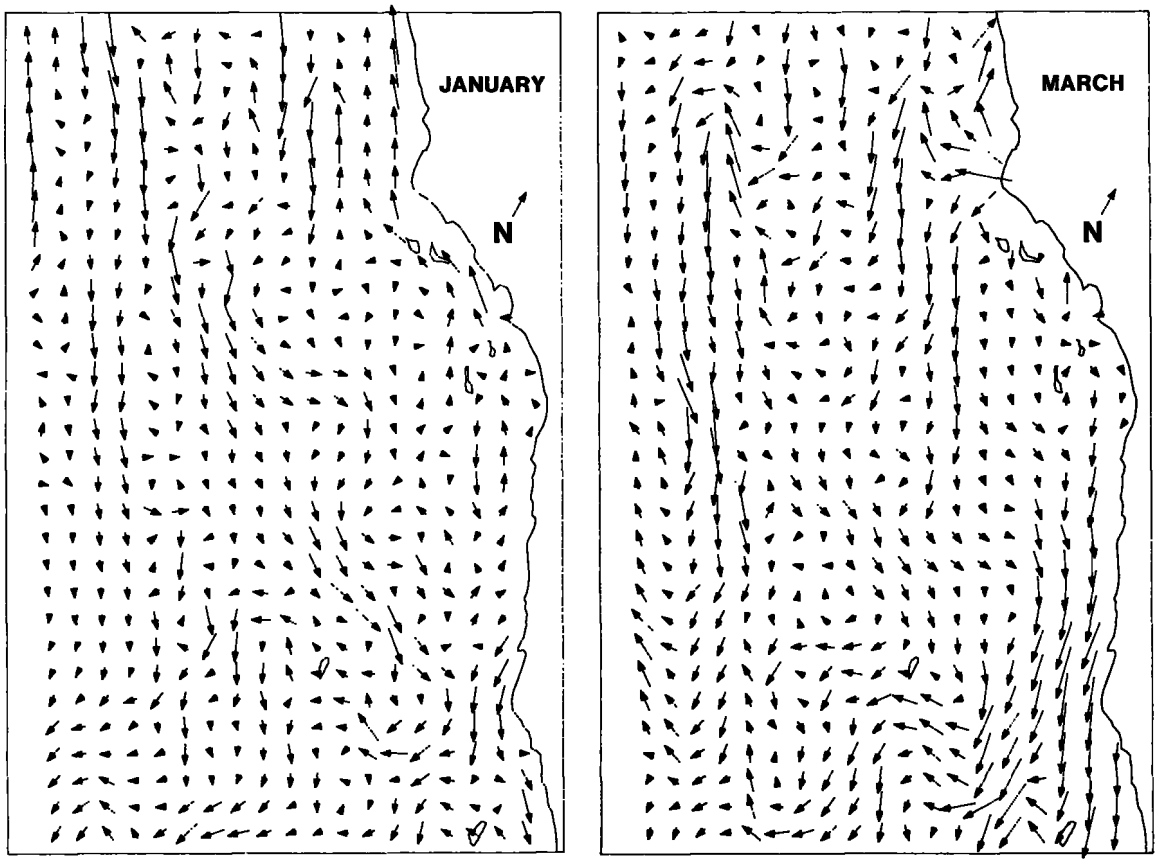

FIGURE 2.—Resultant mean current vectors for the normal January and the March seasonal current data used in this study. See text for cautions concerning figure interpretation. Length of arrow indicating north direction corresponds to a current velocity of 10 cm/s.

producing offshore directed Ekman transport. Two current fields were obtained by increasing the crossshore component of the mean March Ekman velocities by the factors 1.5 and 3.0, and then combining the April seasonal geostrophic and augmented March Ekman velocities. Wind stress, and hence transport, is proportional to the square of wind speed. This means that roughly a 22% increase in a downshore wind speed increases the corresponding offshore directed Ekman transport by the factor 1.5. A threefold increase in offshore Ekman transport results from about a 77% increase in the downshore wind speed. Bakun and Nelson (1976) presented extensive statistical analyses of an "upwelling index" (defined as the offshore directed component of Ekman transport) for the location lat. 33°N, long. 119°W (this point is very close to location A used in the simulations; see below). Over an annual cycle the mean upwelling index for this location changes by at least a factor of two, with a rapid increase in both mean and standard deviation during the spring. The March mean index at this point was about 50 t/s per 100 m of coastline with a standard deviation of roughly 80, hence upwelling at this particular time and location can be highly variable. Further, Bakun and Nelson (1976) found that enhanced or diminished upwelling persists on a seasonal time scale, so incorporation in the model of prolonged increased Ekman transport was not unrealistic.

Diffusion was incorporated into the model solely to parameterize subgrid scale mixing; including larger scale and more ephemeral mixing processes would obscure the broad seasonal trends the model was intended to illustrate. The eddy diffusivity parameter was computed using scale-dependent diffusion formulae of Okubo (1976) and a regression analysis of diffusion data presented by Okubo (1971). The finite-difference representation of diffusion required the use of a pseudo-Fickian diffusivity coefficient, so the mean scale-dependent diffusivity for the 37 km grid spacing ($K_x = K_y = 101$ m^2/s) was

used for all locations and all times in the model. The numerical method incorporated diffusion as the weighting factor $\coth[(uh)/(2K)]$ for the flux at each grid cell interface, where u is the current velocity at the interface and h is the 37 m grid spacing (see Power 1984 for further details). Hence, diffusion becomes important in regions of low current velocity, and at higher velocities diffusion is less important and advection dominates the flux. For the current velocities in most of the modeled region, the above hyperbolic cotangent function is usually evaluated to a magnitude near unity, making the contribution of turbulent transport to larval drift minimal relative to advective (current velocity) transport.

Simulations were carried out by starting an initial point source of northern anchovy eggs or larvae at various locations historically known to be larval anchovy habitat (Hewitt 1980). Examples of simulations for four starting locations (Table 1; Fig. 1), which are representative of the overall patterns produced by the simulations, are presented here. The four locations will be referred to in the text by their letter designations indicated in Figure 1 and Table 1. Northern anchovy larvae begin to school at about 27 d (Hunter and Coyne 1982); therefore larval distributions after 30 d of drift are presented. Thirty-d-old larvae are also rapidly increasing their "patchiness" (Hewitt 1981a), indicating that they could then exert significant control over their position. The time step in the simulations was 1 d. Results from a simulation using the actual northern anchovy egg distribution found in 1982 as the initial condition can be found in MacCall (1983).

TABLE 1.—Geographic and CalCOFI coordinates of starting locations for simulations presented in this paper. Letter designation corresponds to the same locations in Figure 1.

Starting location	Coordinates		CalCOFI	
	Lat. N	Long. W	Line	Station
A	33°08.4′	118°51.4′	89.17	42.5
B	32°54.1′	117°47.3′	92.5	32.5
C	31°59.3′	118°05.4′	95.83	42.5
D	32°14.1′	119°09.2′	92.5	52.5

Northern anchovy larval concentrations in the contour plots are relative to starting concentration; the unitless contour value of 10^{-2} represents a larval concentration two orders of magnitude below the starting concentration, and only concentrations down to 10^{-7} are illustrated. Larvae were permitted to be advected out the borders of the modeled area, except for the border along the coast. Grid cells bordering the Santa Barbara Channel (at about lat. 34°N, long. 120°W; Fig. 1) between the Channel Islands and Point Conception were open, and larvae advected into this region were considered to be lost from the system. Larvae were not permitted to be transported across any of the islands in the modeled region. Because March is the peak spawning time of northern anchovy, the effects of different starting locations on the 30-d larval distributions during March conditions will be presented first. The effects of spawning in different seasons and enhanced offshore Ekman transport during March will then be presented for comparison. The simulation results nominally represent larval northern anchovy distributions, but the results also apply to any planktonic species that begin drift at the same locations and maintain themselves in the top 50 m of the California Current.

The overall extent of onshore-offshore and alongshore transport was of major interest in this study. A convenient way of summarizing the simulated larval distributions relative to their cross-shore distribution was to sum all larval concentrations in the cells having the same CalCOFI station coordinates. These sums were converted to percentages of the total number of larvae at 30 d, and the cumulative percentage of larvae present as one progressed offshore was plotted versus CalCOFI station coordinates. A similar procedures using CalCOFI line coordinates was done to summarize alongshore transport.

RESULTS

Effects of Starting Location, Normal March Currents

Northern anchovy larvae that began drift at location B, near the coast, were transported downshore by March currents (Fig. 3B). This was an effect of the nearshore southeasterly current (Fig. 2), and because of this flow only 15% of the larvae were at or upshore of the starting location after 30 d of drift

FIGURE 3.—Distribution of northern anchovy larvae after 30 d of drift in March currents. Letter designation corresponds to a simulation with northern anchovy begun at the corresponding lettered location in Figure 1 and Table 1; starting location is marked in this and subsequent contour plots with asterisks. Locations A and C share the same CalCOFI station coordinate; points B and D have the same CalCOFI line coordinate. Concentration contour intervals are proportions of the starting concentration, decreasing in order of magnitude steps. Tic marks around perimeter are at whole degrees of latitude and longitude; dots are at intervals of 3.33 CalCOFI line units from lines 70 to 120 and intervals of 10 station units offshore to station 120 (i.e., every 74 km).

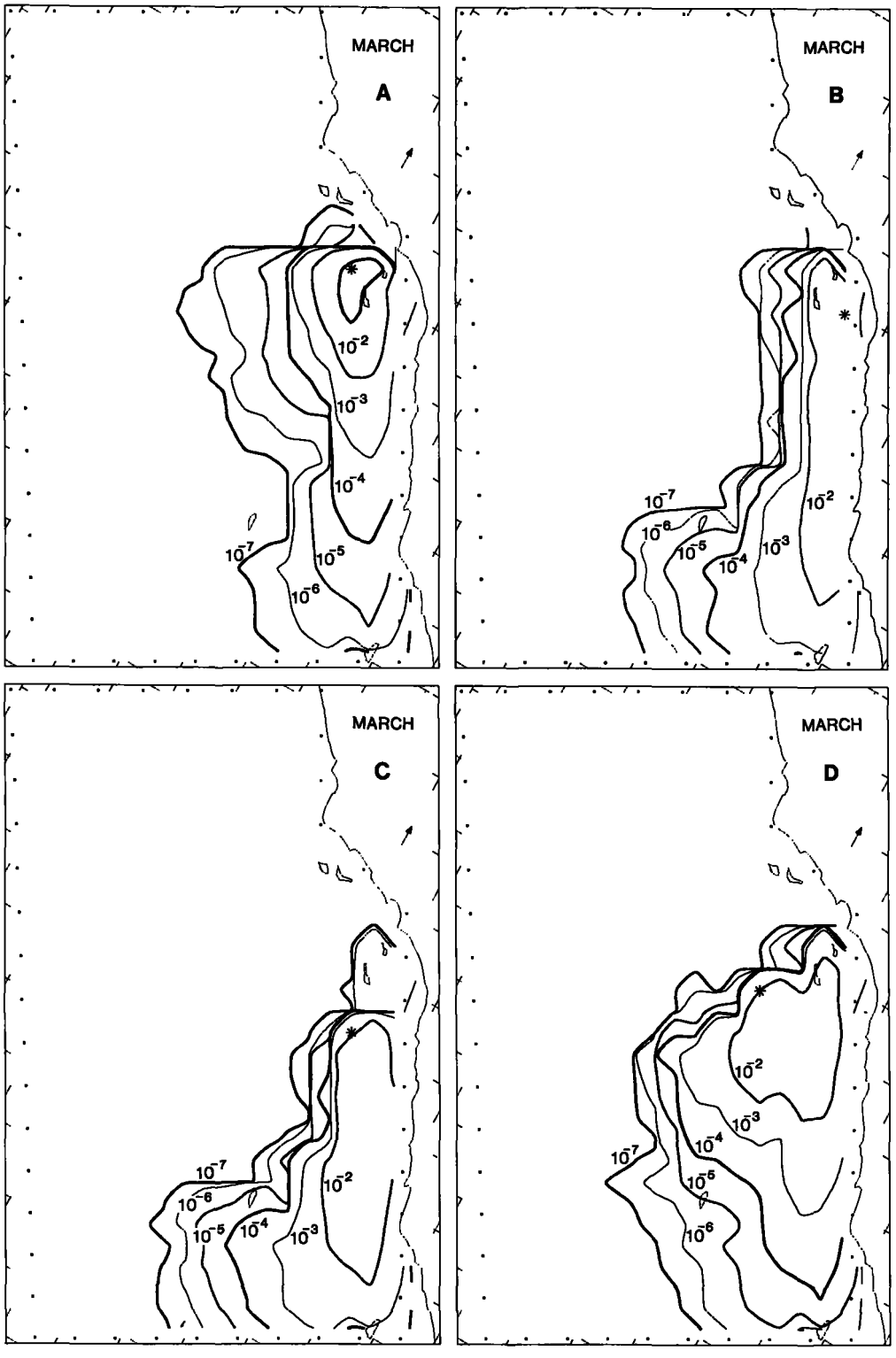
MARCH
A
10^{-2}
10^{-3}
10^{-4}
10^{-5}
10^{-6}
10^{-7}
MARCH
B
10^{-2}
10^{-3}
10^{-4}
10^{-5}
10^{-6}
10^{-7}
MARCH
C
10^{-2}
10^{-3}
10^{-4}
10^{-5}
10^{-6}
10^{-7}
MARCH
D
10^{-2}
10^{-3}
10^{-4}
10^{-5}
10^{-6}
10^{-7}

(Fig. 4). The alongshore distribution of larvae below the starting point was quite uniform, and the lower larval concentrations had reached the southern border of the modeled region (CalCOFI line 120). Dispersal offshore was minimal, and a majority of the larvae lay in a band near the coast with about equal proportions inshore and offshore of the starting point; 92% of the larvae were on or inshore of CalCOFI station 37.5. After initial southeasterly transport, some larvae were transported in an offshore, southwesterly direction.

Extensive downshore transport also occurred to northern anchovy larvae begun at location C, and in fact only 3% of the larvae remained at or upshore of the starting location after 30 d of drift (Figs. 3C, 4). The larvae begun at point C were also concentrated in a narrow band along the coast, but unlike those started at point B most of the larvae begun at C moved inshore of the starting location after 30 d of drift.

Northern anchovy larvae begun at the offshore location D showed much less extensive downshore transport than those begun at B or C (Figs. 3D, 4). Only 10% of the larvae remained at or upshore of the starting point, but 86% of the total remained at or between CalCOFI line 92.5 (location C's line coordinate) and line 102.5, a span of 222 km. Most larvae were inshore of location D, and the cross-shore distribution was slightly more uniform than those begun farther inshore. Starting point D's distance from the coastline permitted the slightly broader cross-shore distribution.

Larvae begun at location A showed an alongshore cumulative percentage distribution after 30 d of drift which was similar to that of larvae that begin drift at point D, although it was displaced farther upshore (Fig. 4). Location A produced the greatest percentage of larvae remaining at or upshore of the starting location, and there is a small patch of high (10^{-1}) larval concentrations present at the starting location (Fig. 3A). This reduced dispersal of larvae begun at A also produced the strongest cross-shore gradient of larvae. A majority of the larvae were again on or inshore of the starting location after 30 d of drift.

In summary, the distributions of northern anchovy larvae that began drift at locations A through D and that were produced by March currents were formed as relatively strong cross-shore gradients, so that the 30-d distributions were bands (ca. 100 km wide) parallel to the coast. The results of starting larvae at locations A, C, and D were that more than 85% of the larvae were inshore of the starting location after 30 d of drift. Larvae that began drift at locations B and C were extensively carried downshore of the starting location. Most of the larvae that started at points A and D also moved downshore from those locations, but the bulk of the larvae were not as widely dispersed from the starting location as those begun at points B and C.

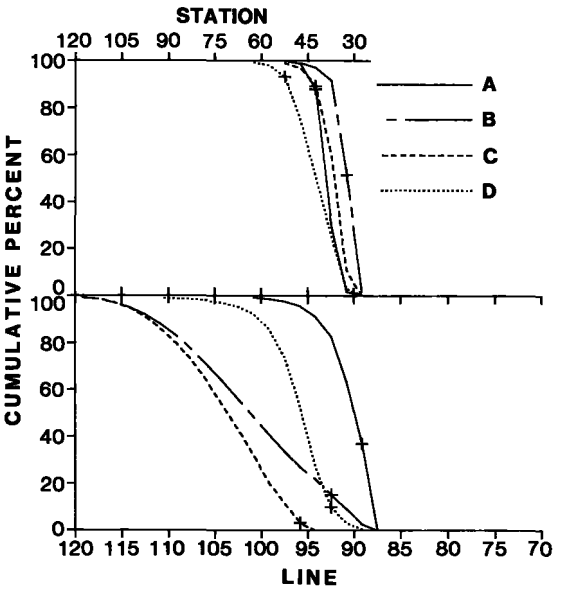

FIGURE 4.—Cumulative percentages of northern anchovy larvae after 30 d of drift, progressing offshore (increasing CalCOFI station number) and downshore (increasing CalCOFI line number), for the four starting locations under March current conditions. Cross symbols are at the starting location's corresponding CalCOFI line or station coordinate. Distance between tic marks on the abscissae is equivalent to a distance of 111 km. Note that a steep curve implies a compact distribution of larvae, while more gradual slopes imply more widely dispersed larvae.

Effects of Seasonal Current Fields on Larval Distribution

The distributions of northern anchovy larvae started at the same location but using different seasonal current regimes appear very different to the eye (Figs. 3, 5-7). Part of this effect is real, but part is also due to displacement of the contours for the lower larval concentrations (e.g., 10^{-7}), which represent few larvae. The cumulative percentage plots (Fig. 8) indicate that, when summarized on a model-wide basis, the overall cross-shore distributions of larvae begun at locations B, C, and D were not greatly different when currents from the four seasonal periods were used in the simulations. A fixed distance offshore there were some large differences in the cumulative percentages among seasons

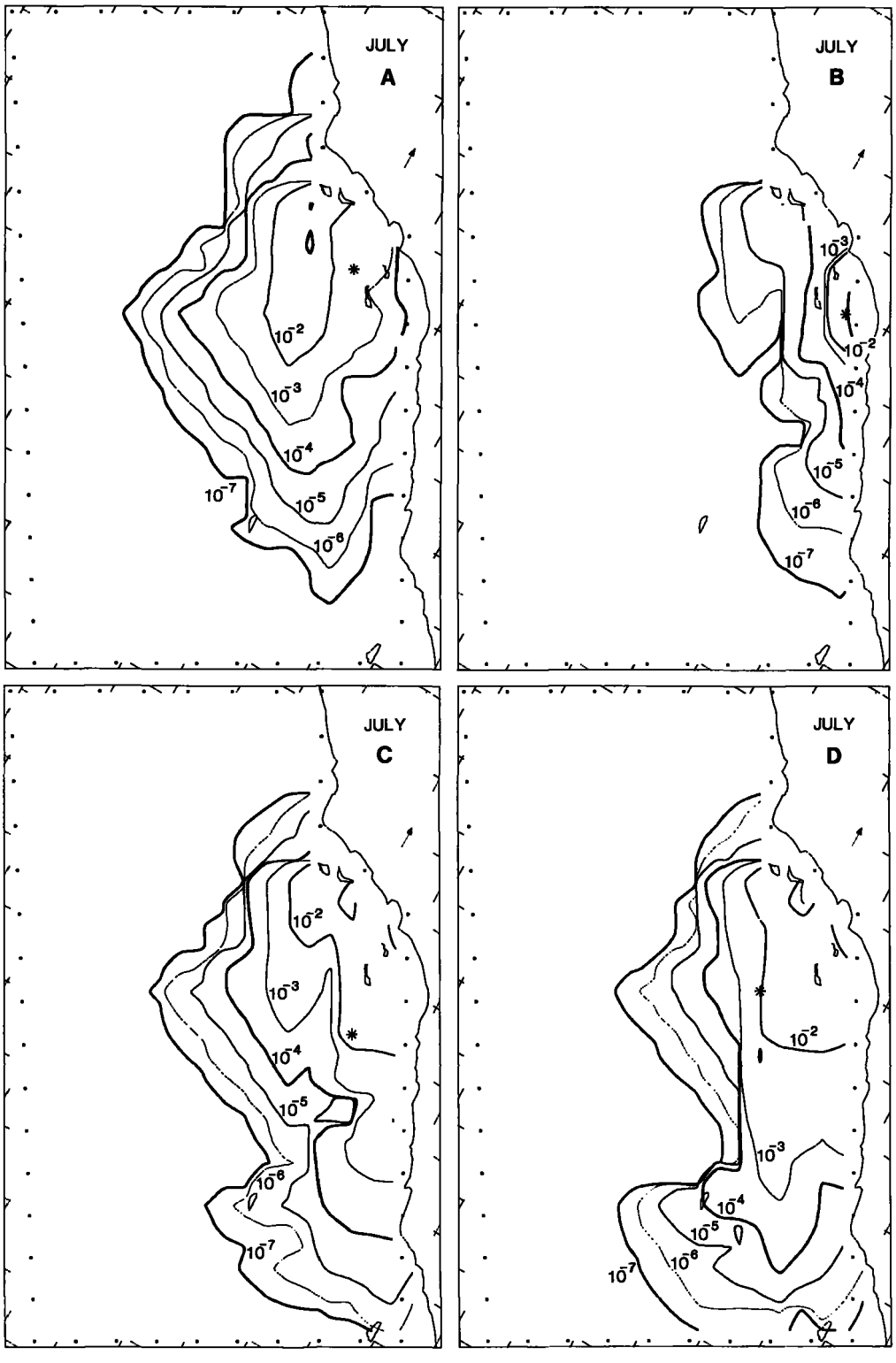

FIGURE 5.—Distribution of northern anchovy larvae after 30 d of drift in normal July currents.

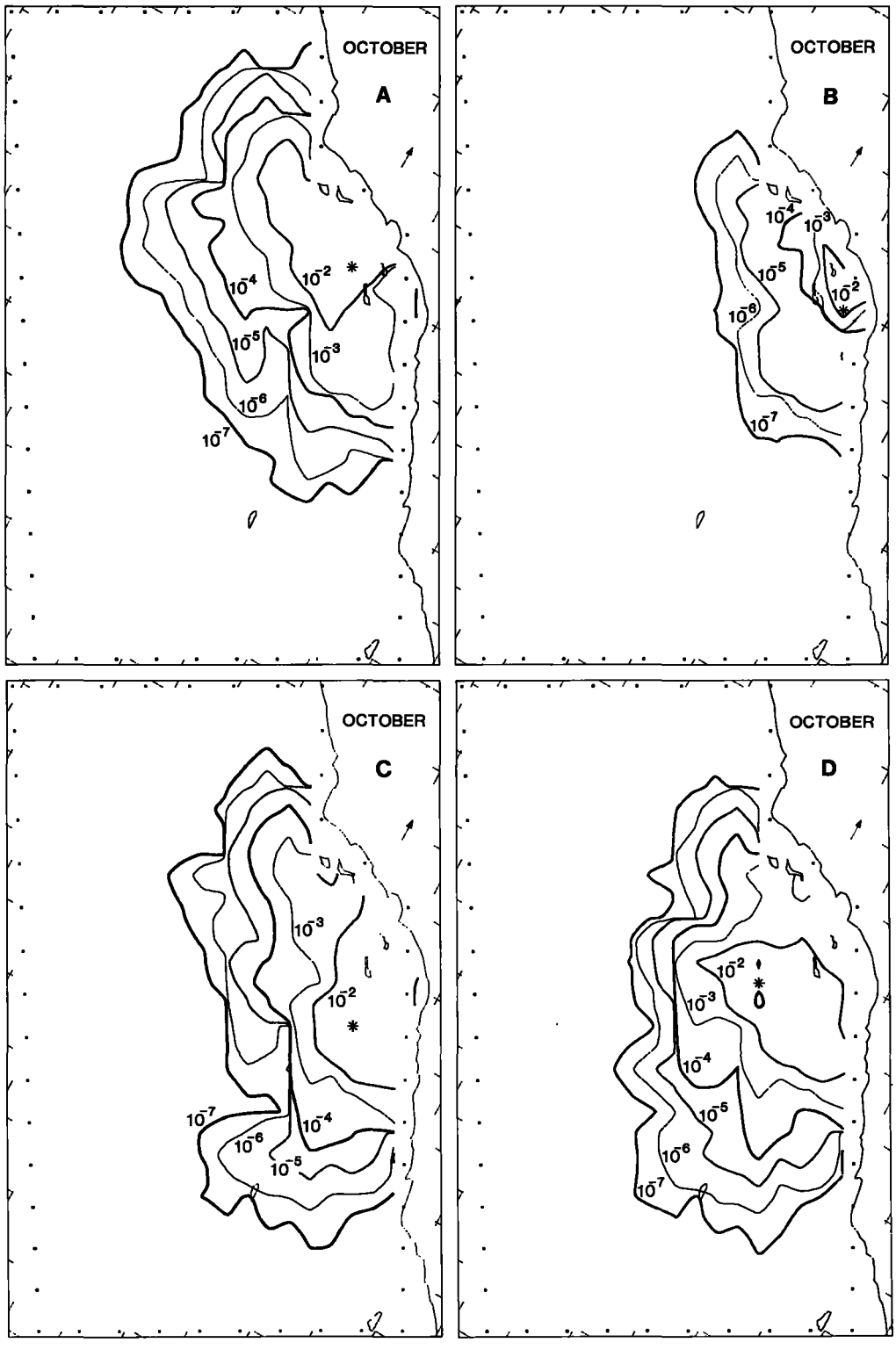

FIGURE 6.—Distribution of northern anchovy larvae after 30 d of drift in normal October currents.

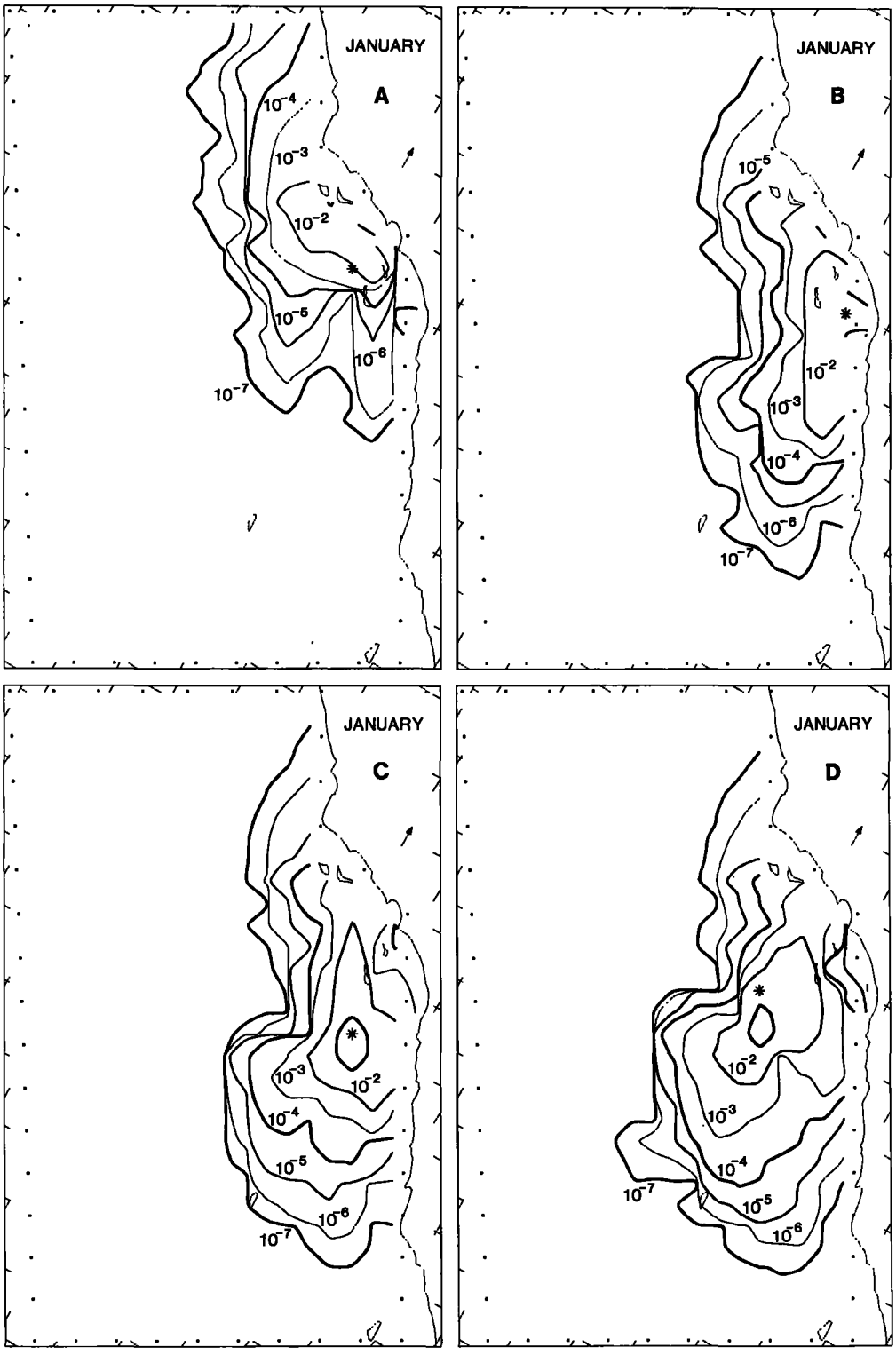

FIGURE 7.—Distribution of northern anchovy larvae after 30 d of drift in normal January currents.

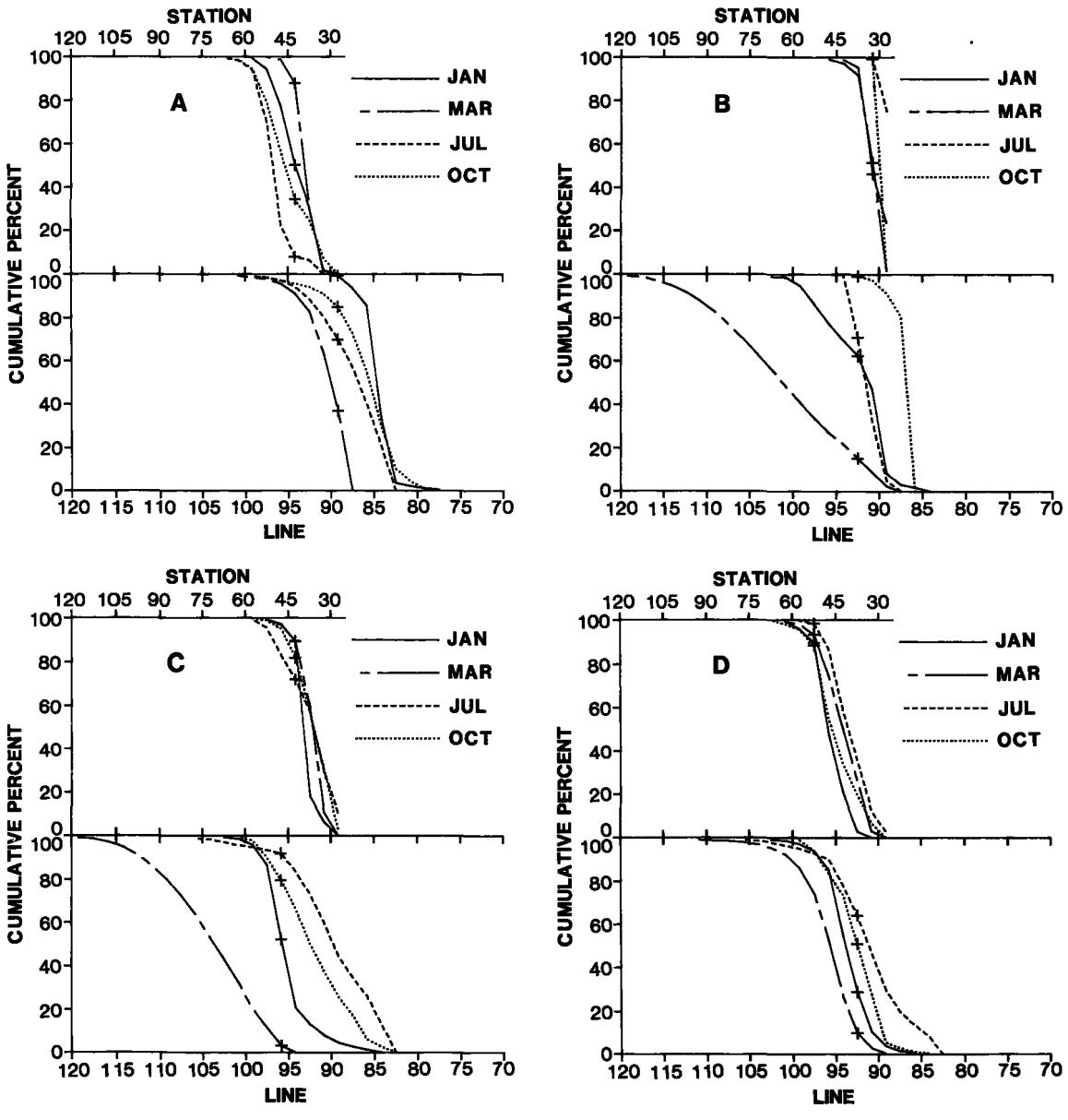

FIGURE 8.—Cumulative percentage plots of northern anchovy larval concentrations after drift in the four seasonal current regimes. Letter designation corresponds to starting locations indicated in Figure 1 and Table 1.

for larvae begun at the same location, but a comparable percentage was usually present a short distance away, i.e., most curves in Figure 8 are closely spaced on the CalCOFI station abscissae. Most larvae begun at the offshore location D moved inshore regardless of season, and the seasonal differences were in the relative extent of inshore movement, the maximum occurring during July. In all simulations the cross-shore distributions of larvae formed strong gradients, regardless of season.

Starting location A is within the Southern California Bight proper, the region that most consistently has high larval concentrations of northern anchovy (cf. Hewitt 1980). Larval distributions started at location A did exhibit notable seasonal differences in their 30-d cross-shore distributions, with the greatest offshore dispersal occurring during July (Figs. 5A, 8A), and the largest inshore movement

occurring during March current conditions (Figs. 3A, 8A). January and October were intermediate between these two extremes. In all cases the cross-shore gradients of larvae were strong.

In contrast, the alongshore distributions of larvae differed markedly when the simulations were done with currents from the four seasonal periods. Virtually all larvae were carried upshore of starting location A by the California Countercurrent in the January simulation (Figs. 7A, 8A), but when the model was run using March currents, a majority of the larvae were downshore of point A after 30 d of drift (Fig. 3A). The July and October simulation results for point A seemed to indicate an annual progression between the March and January extremes (Fig. 8A).

The seasonal differences in the overall alongshore distributions were even more dramatic for northern anchovy larvae begun at locations B and C. The uniform downshore distribution produced by March currents differed from the distributions formed in all other seasons. Larvae begun at location B were all transported upshore of the starting location during October current conditions (Fig. 6B). When January currents were used (Fig. 7B), the upshore movement had lessened, so that only 62% of the larvae were at or upshore of location B, and the larvae were more evenly distributed along the coast (Fig. 8B). March currents yielded the greatest downshore movement, and the July distribution (Fig. 5B) was intermediate between that produced by March and October conditions, with the alongshore gradient of larvae again steepening. The changes on an annual basis between upshore, then downshore transport were similar for larvae begun at location C, except that the July current conditions produced the greatest upshore transport (Figs. 5C, 8C); March again produced the maximum downshore transport for larvae begun at point C (Fig. 3C). Larvae begun at location C formed a relatively compact distribution after 30 d of drift in the January currents (Fig. 7C).

The overall alongshore distributions of northern anchovy larvae that started drift at point D appeared to be least influenced by seasonal changes in the currents, although March conditions again produced the greatest transport downshore of the starting point (Fig. 3D), with July currents again yielding the greatest upshore transport (Fig. 5D). January currents also produced a very compact distribution of larvae started at location D, similar to that of larvae begun at point C.

In summary, only northern anchovy larvae begun at location A appeared to have notable differences in their model-wide, cross-shore distributions after 30 d of drift. Larvae begun at all four locations did have substantial seasonal differences in their alongshore distributions, with March currents consistently producing the greatest downshore dispersal. The least downshore dispersal occurred during January, October, July, and July current conditions for larvae started at locations A, B, C, and D respectively. January currents generally seemed to produce the most compact 30-d distributions of larvae (least dispersal).

Effects of Increased Offshore Ekman Transport, March Currents

Increasing the March cross-shore Ekman transport by a factor of 1.5 had little effect on the 30-d distributions of northern anchovy larvae begun at locations B and C (Fig. 9); these curves are also closely spaced on the CalCOFI station abscissae. Increasing the average or "normal" offshore Ekman component by a factor of three produced more noticeable changes in the cross-shore distributions of larvae begun at points B and C, but this effect was not substantial; the contours representing the lower concentrations extended far offshore (Fig. 10B, C), but the higher concentration contours, which delimit the majority of the larvae, were not greatly displaced from those of normal March currents (Fig. 3B, C). This is also evident in the cumulative percentage curves.

In comparison, northern anchovy larvae begun at locations A and D underwent about the same increase in offshore dispersal with a 1.5× offshore directed Ekman component increase as those begun at points B and C did with the 3× offshore Ekman increase (Fig. 9). When the offshore directed Ekman transport was increased to three times its normal mean value, the effects on larvae begun at points A and D were substantial. A majority of the larvae were carried offshore of starting locations A and D, and a large fraction were transported a significant distance (Fig. 10A, D), well seaward of the Southern California Bight. The increase in offshore Ekman transport also noticeably affected the alongshore distributions of larvae begun at locations A and D (Fig. 9). The overall pattern of alongshore distribution is similar to that produced by the normal mean conditions, but the larvae were generally farther downshore.

DISCUSSION

Models have inherent assumptions and simplifica-

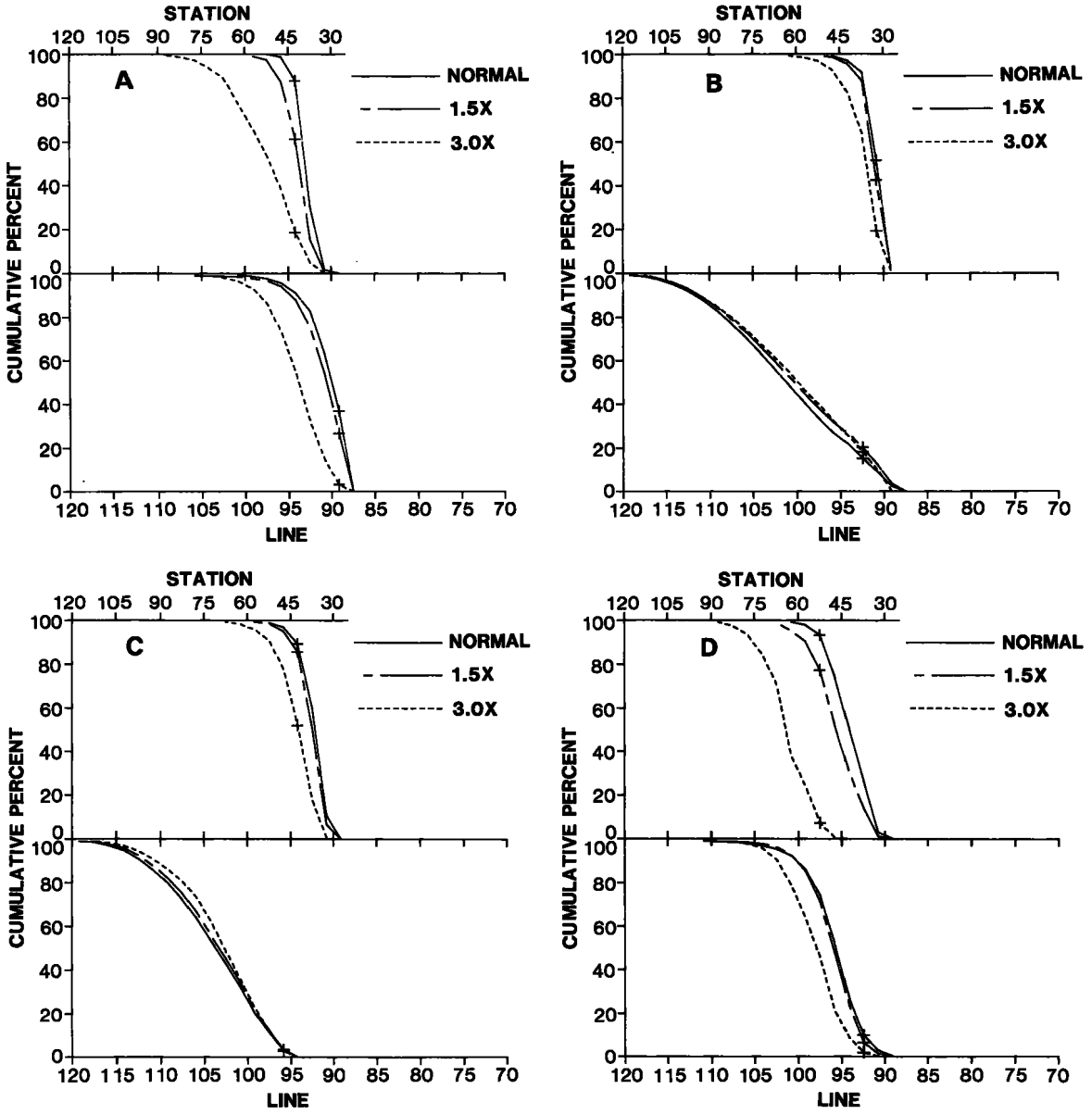

FIGURE 9.—Cumulative percentage plots of northern anchovy larval concentrations after 30 d drift in the three March Ekman current regimes ("normal" or long-term mean, 1.5× offshore directed Ekman transport, 3× offshore directed Ekman).

tions, and thus approximate what occurs in nature. The geostrophic current information, while some of the best available, nonetheless constrained the spatiotemporal resolution of this model, and incorporating Ekman transport required several assumptions. Further, there can be considerable interannual variability in the modeled region (Mooers and Robinson 1984; Simpson et al. 1984), and presumably the model is of "average" conditions and cannot be representative of any specific year; I felt that including such variability (assuming adequate data were available) would complicate the results without significantly contributing to biological insight. An

FIGURE 10.—Distribution of northern anchovy larvae after 30 d of drift in March currents with three times the normal offshore directed Ekman transport.

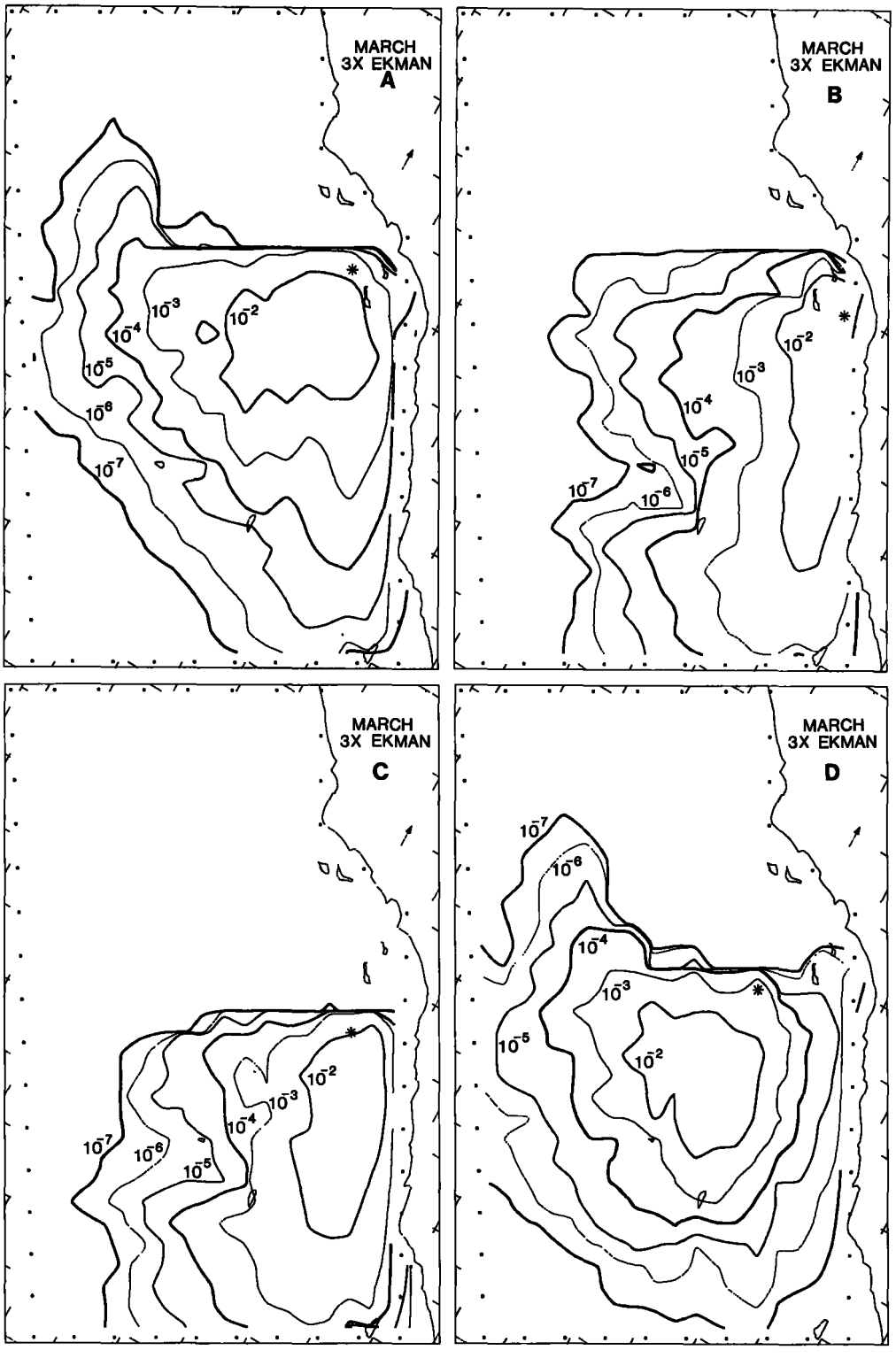
MARCH
3X EKMAN
A
10^{-2}
10^{-3}
10^{-4}
10^{-5}
10^{-6}
10^{-7}
MARCH
3X EKMAN
B
10^{-2}
10^{-3}
10^{-4}
10^{-5}
10^{-6}
10^{-7}
MARCH
3X EKMAN
C
10^{-2}
10^{-3}
10^{-4}
10^{-5}
10^{-6}
10^{-7}
MARCH
3X EKMAN
D
10^{-2}
10^{-3}
10^{-4}
10^{-5}
10^{-6}
10^{-7}

additional confounding factor is the lack of biological information in the model; consistent larval behavior patterns (e.g., diurnal vertical migrations) and spatially heterogeneous mortality could produce distributional patterns differing from those presented here. In spite of these caveats, the simulations do demonstrate that variations in northern anchovy spawning location and time, and changes in the magnitude of offshore directed Ekman transport, can have significant consequences for the subsequent larval distribution. By inference, these changes in distribution can result in increased or reduced larval mortality, and ultimately affect adult northern anchovy population size.

Offshore transport was not significant in the simulations done with the unaugmented or "normal" March (seasonal April geostrophic + March Ekman) currents. A majority of the northern anchovy larvae that began drift at the four starting locations were inshore of their starting points after 30 d of drift, and the cross-shore distributions indicated that most larvae occupied a relatively narrow range of distances close to shore. Mais (1974) and Methot (1981) reported that most juvenile northern anchovy occupy inshore areas in the fall, and the model indicates that this inshore movement could be facilitated by passive drift. As mentioned earlier, the consensus is that nearshore regions provide more hospitable food conditions for the northern anchovy larvae. Lasker (1978, 1981) summarized the results of surveys of larval food distributions in the Southern California Bight. His figures indicate that suitable larval food concentrations decline rapidly as one progresses offshore. O'Connell (1980) reported the results of a survey for starving northern anchovy larvae in the Southern California Bight, the degree of starvation being defined by histological criteria. He found apparently healthy larvae at locations as far as about 250 km offshore (at lat. 32°30'N, long. 120°W), where model concentrations were $<10^{-7}$ after 30 d in all March simulations except for larvae begun at A, where they were $<10^{-4}$. Despite the good condition of these offshore larvae, the simulation results indicate a low likelihood of their being recruited to the nearshore juvenile population. The low offshore larval concentrations will also hinder the development of schooling (Hewitt 1981a).

The minimal offshore transport situation found in the March current simulations was also generally true when simulations were done using currents from other seasons, except for northern anchovy larvae begun at location A. This point is the most interior starting location within the Southern California Bight proper and is primary northern anchovy spawning habitat (Hewitt 1980) and where seasonal changes in the currents are especially important (Tsuchiya 1980). Spring is a time when currents in the Southern California Bight are not as well organized as other times of the year, and the Southern California Eddy is often absent (Hickey 1979; Owen 1980). It is interesting that currents during March, the peak spawning period, produced the least offshore transport of larvae begun at location A when compared with other seasons, even though March is the time of greatest overall Ekman transport (Bakun and Nelson 1976). There is significant spawning in January (Methot 1981), and the January simulations also had reduced dispersal of larvae. The model results support the hypothesis of Parrish et al. (1981) that northern anchovy spawning in the Southern California Bight do so at a time and place that minimizes offshore transport of eggs and larvae.

It is clear that the overall 30-d alongshore distributions of northern anchovy larvae produced by normal March currents depended largely on the spawning location's proximity to the well-defined southeasterly current present near the coast in the southern half of the modeled region. Larvae that started drift near this current underwent extensive downshore transport. Larvae begun farther into the Southern California Bight (location A), and farther offshore (location D), were also transported downshore, but to a much lesser extent. This again confirms the role of the Southern California Bight as an area where minimal transport of spawning products takes place. The southwesterly, offshore transport that occurred in many of the simulations at the southern margin of the modeled region (between CalCOFI lines 110 and 120) is consistent with the evidence that this region forms a faunal boundary between species of the Southern California Bight and those of Baja California to the south, and that this faunal boundary is created by current patterns (Hewitt 1981b). This is also a region of increased surface convergence (Parrish et al. 1981).

The extent of alongshore transport was markedly different for northern anchovy larvae begun at the same starting location when currents from the different seasons were used. Depending on starting location, seasonal changes in currents could produce almost complete reversals between predominantly upshore or downshore transport. March currents consistently produced the greatest downshore transport. These effects were due to the presence or absence of the Southern California Eddy and the Southern California Countercurrent. Because the Southern California Countercurrent is present

year-round, except during peak spawning in the spring, it is clear that the relationship between the time of northern anchovy spawning and the time that this countercurrent diminishes is critical. The simulations indicated that eggs and larvae from early spawning (i.e., January) are carried upshore into the Santa Barbara Channel and north of Point Conception, while those from later spawning (March) move in the opposite, southeasterly direction. The sizes and birth dates of juveniles collected in the fall of 1978 and 1979 were in accordance with this pattern. Methot (1981) reported that juvenile northern anchovy collected during both fall seasons in the northern portion of the Southern California Bight had birth dates (as determined from daily growth increments in otoliths) in the preceding months of December and January, and these fish were generally larger than those collected farther to the south. The northern anchovy collected in the south had predominantly February and March birth dates. It may be that the northern group, containing fish from early spawning, were advected to the north by the Southern California Countercurrent and that the southern group of fish from late spawning were produced when the surface countercurrent had diminished. Future studies of the transport and distribution of northern anchovy larvae or other planktonic species in the Southern California Bight should incorporate as much information as is available on the presence and magnitude of the Southern California Countercurrent and the Southern California Eddy.

Nearshore winds in the Southern California Bight are relatively weak, and downshore wind speeds generally increase farther offshore (Bakun and Nelson 1976; Nelson 1977; Dorman 1982). The implication, in terms of offshore transport, is that larvae closest to shore are affected least by offshore transport, while those farther offshore experience a much greater impact. Thus the areal extent of northern anchovy spawning interacts with offshore Ekman transport; in years when most northern anchovy spawn close to shore there will be decreased offshore transport, because of weak inshore winds, than in years when northern anchovy spawn farther offshore. The impact on the products of offshore spawning will depend on the magnitude of the winds in the offshore areas in each particular year. Northern anchovy larvae that began drift farthest north in the Southern California Bight (location A) and at the more offshore location (D) were most affected by increases in offshore directed Ekman transport, indicating southerly and inshore spawning are best for reduced dispersal in March. Hewitt and Methot (1982) stated that the area of northern anchovy spawning was more compact and more northerly in 1978 than in 1979. Survival of young larvae was about the same in both years, indicating that early mortality from starvation and predation was not substantially different in the two years. Survival through the juvenile stage was greater in 1978 than in 1979, however, and Hewitt and Methot (1982) cited increased offshore transport in 1979 as a possible reason.

Superimposed on the effects of spawning location is the interaction between the increase in downshore wind speeds (offshore directed Ekman transport) as one progresses offshore and the magnitude of interannual variations in the wind speeds. In the simulations the effects of the 3× increase in Ekman transport were substantially greater than those of the 1.5× increase. The 1.5× change was not a great enough increase to carry many northern anchovy larvae into offshore regions of higher, offshore directed Ekman transport. The inshore 3× increase carried a greater fraction of larvae farther offshore, and the 3× increase in the offshore region subsequently operated on a greater proportion of the larval population. Thus there was an interaction between enhanced offshore directed Ekman transport in the nearshore area and increased Ekman transport farther offshore, the two of these acting together to produce the extensive drift evident in the simulation results. Years in which downshore winds increase in only the inshore or the offshore regions would not produce as much overall offshore dispersal. Bakun and Nelson's (1976) statistical analyses of the "upwelling index" indicates that prolonged increased Ekman transport is feasible, although the 3× condition would probably be a particularly bad year. It should also be noted that Ekman transport was incorporated into the model as acting uniformly on the 50 m surface layer, and presumably the model depicts the drift of "average" larvae. Larvae that remain near the surface or at 50 m would undergo greater or lesser transport, respectively. Alternatively, it is known that winds in the Southern California Bight have a strong diurnal periodicity (Bakun and Nelson 1976; Dorman 1982), and a diurnal vertical migration coupled with diurnal changes in the winds could significantly alter larval drift.

In summary, the simulation results indicated that seaward dispersal of northern anchovy larvae is generally small, but that seasonal effects are strongest in the area of peak spawning (location A) and that March spawning at this point minimizes offshore dispersal. Spawning at locations or times near

well-defined currents, such as the California Countercurrent, can produce major changes in larval distribution, and consequently may affect larval survival. The effect of offshore directed Ekman transport on the larval population depends on the areal extent of northern anchovy spawning, and the spatial distribution of any changes in wind stress and subsequent Ekman transport; an increase in Ekman transport in both the inshore and offshore regions will act together to produce maximum offshore dispersal.

ACKNOWLEDGMENTS

This work was done while the author held a National Research Council Research Associateship. I thank Reuben Lasker and John Hunter for their hospitality and advice, as well as for the opportunity to conduct this research. Larry Eber and Craig Nelson were instrumental in providing dynamic height and wind speed data, without which this work could not have been done. I also thank Andy Bakun, Roger Hewitt, Ron Lynn, Alec MacCall, Rick Methot, Bob Owen, Dick Parrish, and Paul Smith for their stimulating discussions, advice, and review of this work. This manuscript was revised while the author held a CIMAS (Cooperative Institute for Marine and Atmospheric Sciences) postdoctoral fellowship at the University of Miami, and this support is gratefully acknowledged.

LITERATURE CITED

AHLSTROM, E. H.
1959. Vertical distribution of pelagic fish eggs and larvae off California and Baja California. Fish. Bull., U.S. 60:107-146.

AKIMA, H.
1978. A method of bivariate interpolation and smooth surface fitting for irregularly distributed data points. ACM Trans. Math. Software 4:148-159.

AMOROCHO, J., AND J. J. DEVRIES.
1980. A new evaluation of the wind stress coefficient over water surfaces. J. Geophys. Res. 85C:433-442.
1981. Reply to comment on 'A new evaluation of the wind stress coefficient over water surfaces'. J. Geophys. Res. 86C:4308.

BAILEY, K. M.
1981. Larval transport and recruitment of Pacific hake *Merluccius productus*. Mar. Ecol. Prog. Ser. 6:1-9.

BAKUN, A., AND C. S. NELSON.
1976. Climatology of upwelling related processes off Baja California. Calif. Coop. Oceanic Fish. Invest. Rep. 19:107-127.

BAKUN, A., AND R. H. PARRISH.
1982. Turbulence, transport, and pelagic fish in the California and Peru Current systems. Calif. Coop. Oceanic Fish. Invest. Rep. 23:99-112.

DORMAN, C. E.
1982. Winds between San Diego and San Clemente Islands. J. Geophys. Res. 87C:9636-9646.

HEWITT, R.
1980. Distributional atlas of fish larvae in the California Current region: northern anchovy, *Engraulis mordax* Girard, 1966 through 1979. Calif. Coop. Oceanic Fish. Invest. Atlas 28, 101 p.
1981a. The value of pattern in the distribution of young fish. Rapp. P.-v. Réun. Cons. int. Explor. Mer 178:229-236.
1981b. Eddies and speciation in the California Current. Calif. Coop. Oceanic Fish. Invest. Rep. 22:96-98.

HEWITT, R. P., AND R. D. METHOT, JR.
1982. Distribution and mortality of northern anchovy larvae in 1978 and 1979. Calif. Coop. Oceanic Fish. Invest. Rep. 23:226-245.

HICKEY, B. M.
1979. The California Current system - hypotheses and facts. Prog. Oceanogr. 8:191-279.

HUNTER, J. R.
1981. Feeding ecology and predation of marine fish larvae. *In* R. Lasker (editor), Marine fish larvae, p. 33-77. Univ. Wash. Press., Seattle-Lond.

HUNTER, J. R., AND K. M. COYNE.
1982. The onset of schooling in northern anchovy larvae, *Engraulis mordax*. Calif. Coop. Oceanic Fish. Invest. Rep. 23:246-251.

HUSBY, D. M., AND C. S. NELSON.
1982. Turbulence and vertical stability in the California Current. Calif. Coop. Oceanic Fish. Invest. Rep. 23:113-129.

LASKER, R.
1978. The relation between oceanographic conditions and larval anchovy food in the California Current: identification of factors contributing to recruitment failure. Rapp. P.-v. Réun. Cons. int. Explor. Mer 173:212-230.
1981. Factors contributing to variable recruitment of the northern anchovy (*Engraulis mordax*) in the California Current: Contrasting years, 1975 through 1978. Rapp. P.-v. Réun. Cons. int. Explor. Mer 178:375-388.

LYNN, R. J., K. A. BLISS, AND L. E. EBER.
1982. Vertical and horizontal distributions of seasonal mean temperature, salinity, sigma-t, stability, dynamic height, oxygen, and oxygen saturation in the California Current, 1950-1978. Calif. Coop. Oceanic Fish. Invest. Atlas 30, 513 p.

MACCALL, A. D.
1983. Population models of habitat selection, with application to the northern anchovy. Ph.D. Thesis, Univ. California at San Diego, San Diego, 170 p.

MAIS, K. F.
1974. Pelagic fish surveys in the California Current. Calif. Dep. Fish Game Fish Bull. 162, 79 p.

MESSERSMITH, J. D., AND ASSOCIATES.
1969. The northern anchovy (*Engraulis mordax*) and its fishery, 1965-1968. Calif. Dep. Fish Game Fish Bull. 147, 102 p.

METHOT, R. JR.
1981. Growth rates and age distributions of larval and juvenile northern anchovy, *Engraulis mordax*, with inferences on larval survival. Ph.D. Thesis, Univ. California at San Diego, San Diego, 203 p.

MOOERS, C. N. K., AND A. R. ROBINSON.
1984. Turbulent jets and eddies in the California Current and inferred cross-shore transports. Science 223:51-53.

NELSON, C. S.
1977. Wind stress and wind stress curl over the California Current. U.S. Dep. Commer., NOAA Tech. Rep. NMFS

SSRF-714, 87 p.

NEUMANN, G., AND W. J. PIERSON, JR.
1966. Principles of physical oceanography. Prentice-Hall, Englewood Cliffs, NJ, 545 p.

O'CONNELL, C. P.
1980. Percentage of starving northern anchovy, *Engraulis mordax*, larvae in the sea as estimated by histological methods. Fish. Bull., U.S. 78:475-489.

OKUBO, A.
1971. Oceanic diffusion diagrams. Deep-Sea Res. 18:789-802.
1976. Remarks on the use of 'diffusion diagrams' in modeling scale-dependent diffusion. Deep-Sea Res. 23:1213-1214.

OWEN, R. W.
1980. Eddies of the California Current system: physical and ecological characteristics. *In* D. M. Power (editor), The California Islands: Proceedings of a Multidisciplinary Symposium, p. 237-263. Santa Barbara Mus. Nat. History.

PARRISH, R. H., C. S. NELSON, AND A. BAKUN.
1981. Transport mechanisms and reproductive success of fishes in the California Current. Biol. Oceanogr. 1:175-203.

POWER, J. H.
1984. A numerical method for simulating plankton transport. Ecol. Model. 23:53-66.

ROTHSCHILD, B. J., E. D. HOUDE, AND R. LASKER.
1982. Causes of fish stock fluctuations: Problem setting and perspectives. *In* B. J. Rothschild and C. Rooth (editors), Fish ecology III, p. 39-86. Univ. Miami Tech. Rep.

SIMPSON, J. J., C. J. KOBLINSKY, L. R. HAURY, AND T. D. DICKEY.
1984. An offshore eddy in the California Current system: preface. Prog. Oceanogr. 13:1-4.

SMITH, P. E.
1972. The increase in spawning biomass of northern anchovy, *Engraulis mordax*. Fish. Bull., U.S. 70:849-874.

SMITH, P. E., AND R. LASKER.
1978. Position of larval fish in an ecosystem. Rapp. P.-v. Réun. Cons. int. Explor. Mer 173:77-84.

SOUTAR, A., AND J. D. ISAACS.
1974. Abundance of pelagic fish during the 19th and 20th centuries as recorded in anaerobic sediments off the Californias. Fish. Bull., U.S. 72:257-273.

STAUFFER, G. D., AND R. L. CHARTER.
1982. The northern anchovy spawning biomass for the 1981-82 California fishing season. Calif. Coop. Oceanic Fish. Invest. Rep. 23:15-19.

SUNADA, J. S.
1975. Age and length composition of northern anchovies, *Engraulis mordax*, in the 1972-73 season California anchovy reduction fishery. Calif. Fish Game 61:133-143.

TSUCHIYA, M.
1980. Inshore circulation in the Southern California Bight, 1974-1977. Deep-Sea Res. 27A:99-118.

VROOMAN, A. M., P. A. PALOMA, AND J. R. ZWEIFEL.
1981. Electrophoretic, morphometric, and meristic studies of subpopulations of northern anchovy (*Engraulis mordax*). Calif. Fish Game 67:39-51.